

Supplementary information

Fast synthesis of polyanionic materials for sodium-ion storage

Jingyuan Zhang, Zeyu Cao, Ying Yang, Zhuo Zheng, Zixian Wang, Hang Ren, Jinyao Yang, Guoyin Zhu, Yizhou Zhang, and Shengyang Dong*

Jiangsu Key Laboratory of New Energy Devices & Interface Science, School of Chemistry and Materials Science, Nanjing University of Information Science and Technology, Nanjing 210044, China.

Experimental section

Preparation of $\text{NaTi}_2(\text{PO}_4)_3$ (NTP).

Citric acid (4 mmol), ammonium dihydrogen phosphate (9 mmol), sodium acetate (3 mmol), and tetrabutyl titanate (6 mmol) were dissolved in 30 mL of deionized water at room temperature and stirred until a homogeneous and transparent precursor solution was formed. The precursor solution was first dried at 80 °C to form a gel-like substance, followed by vacuum drying at 100 °C to obtain the precursor powder.

UHS method: The precursor powder was then ground uniformly and pressed into a precursor disc with a diameter of 10 mm and a thickness of approximately 1 mm using a pellet press. The precursor disc was sandwiched between two graphite papers and subsequently placed in the Joule heating device, where it was sintered for 10 s at temperatures ranging from 550 to 920 °C.

Traditional method: The precursor powder was thoroughly ground and then placed in a tube furnace. Under an argon atmosphere, it was first sintered at 450 °C for 4 hours, followed by sintering at 750 °C for 8 hours, with a heating rate of 5 °C min⁻¹.

Preparation of $\text{Na}_3\text{V}_2(\text{PO}_4)_3$ (NVP).

Vanadium pentoxide (2 mmol), anhydrous oxalic acid (6 mmol), glucose (1 mmol), sodium oxalate (3 mmol), and ammonium dihydrogen phosphate (6 mmol) were dissolved in 20 mL of deionized water and stirred in a water bath at 80 °C to form a blue Solution A. Meanwhile, carbon nanotubes were dispersed in 20 mL of ethylene glycol via ultrasonication to form a homogeneous Solution B, which was subsequently added to Solution A. The mixture was continuously stirred until a uniform precursor solution was obtained. The precursor solution was then dried at 100 °C to form a gel-like substance, followed by vacuum drying at 120 °C to obtain the precursor powder. The precursor powder was then ground uniformly and pressed into a precursor disc with a diameter of 10 mm and a thickness of approximately 1 mm using a pellet press. The precursor disc was sandwiched between two graphite papers and subsequently placed in the Joule heating device, where it was sintered for 10 s at temperatures ranging from 550 to 930 °C.

Preparation of $\text{Na}_2\text{VTi}(\text{PO}_4)_3$ (NVTP).

Sodium oxalate (8 mmol), ammonium metavanadate (4 mmol), and ammonium dihydrogen phosphate (12 mmol) were dissolved in 30 mL of a 0.2 mol/L citric acid solution under stirring to form a homogeneous Solution A. tetrabutyl titanate (4 mmol) was dissolved in 30 mL of ethanol under stirring to form a homogeneous Solution B. Solution B was then added to Solution A, and the mixture was continuously stirred until a uniform precursor solution was obtained. The precursor solution was dried at 80 °C to obtain the precursor powder. The precursor powder was then ground uniformly and pressed into a precursor disc with a diameter of 10 mm and a thickness of approximately 1 mm using a pellet press. The precursor disc was sandwiched between two graphite papers and subsequently placed in the Joule heating device, where it was sintered for 10 s at temperatures ranging from 550 to 940 °C.

Electrochemical measurements

In the organic electrolyte system, the NTP electrode was prepared by the active materials, conductive carbon (Super P) and polyvinylidene fluoride (PVDF) in the weight ratio of 8:1:1. The slurry was coated on Cu foil and dried in vacuum at 80 °C for 12 h, resulting in an active material load of 1-1.5 mg cm⁻². The NVP and NVTP electrode were prepared by the active materials, carbon black (KETJEN BLACK EC600JD) and polyvinylidene fluoride (PVDF) in the weight ratio of 8:1:1. The slurry was coated on Al foil and dried in vacuum at 80 °C for 12 h. CR2032-type coin cells were assembled in an argon-filled glovebox. Na-metal foil use as counter electrode, and 1.0 M NaPF₆ dissolved in DIGLYME as electrolyte.

In the aqueous electrolyte system, the NTP electrode was prepared by the active materials, conductive carbon (Super P) and polyvinylidene fluoride (PVDF) in the weight ratio of 8:1:1. The slurry was coated on a 10 mm diameter carbon paper and dried in vacuum at 80 °C for 12 h, resulting in an active material load of 1-1.5 mg cm⁻². The counter electrode used was activated carbon (AC) films, in which AC, carbon black, and polytetrafluoroethylene (PTFE) were blended with a mass ratio of 8:1:1. The Ag/AgCl electrode (1 M KCl) was used the reference electrode. All half-cell electrochemical tests were tested in three-electrode cells, and 1.0 M NaAc dissolved in deionized water as electrolyte.

The cyclic voltammetry (CV) and electrochemical impedance spectroscopy (EIS)

were tested on a CorrTest CS-350 electrochemical workstation. The galvanostatic charge-discharge (GCD) and the galvanostatic intermittent titration technique (GITT) process were carried out on LANBTS cell test system at room temperature.

A quantitative analysis of the relationship between the peak current (i , $\text{A}\cdot\text{g}^{-1}$) and the scan rate (v , $\text{mV}\cdot\text{s}^{-1}$) in CV curves were performed using Equation (S1), which establishes a linear correlation between $\log i$ and $\log v$:

$$i = av^b \quad (\text{S1})$$

Here, a is a constant, and b represents the slope of the linear fit obtained by plotting $\log i$ versus $\log v$.

To quantitatively calculate the contributions of capacitive-controlled (k_1v) and diffusion-controlled ($k_2v^{1/2}$) processes at different scan rates, Equation (S2) is applied:

$$i = k_1v + k_2v^{1/2} \quad (\text{S2})$$

This allows for the determination of the proportional contributions of capacitive and diffusion-controlled components. Then the ratio of capacitance contribution can then be figured out.

The GITT was employed to figure out the diffusion coefficient of Na^+ by using a set of galvanostatic discharge pulses of 10 min at a current density of 100 mA g^{-1} , followed by relaxing one hour.

The GITT process involves applying a short galvanostatic current pulse followed by a relaxation period, where the relaxation time is significantly longer than the pulse duration. In this work, the pulse duration τ (s) is set to 600 s, and the relaxation time is 1 h. The potential E (V) versus time t (s) curve obtained from the Galvanostatic Intermittent Titration Technique (GITT) experiments allows the determination of the carrier diffusion coefficient D ($\text{cm}^2\cdot\text{s}^{-1}$) using Equation (S3):

$$D = \frac{4}{\pi\tau} \left(\frac{m_b V_m}{M_b S} \right)^2 \left(\frac{\Delta E_s}{\tau (dE_\tau / d\sqrt{\tau})} \right)^2 \quad (\tau \ll L^2/D) \quad (\text{S3})$$

In Equation (S3): m_b (g) is the active mass of the electrode, M_b ($\text{g}\cdot\text{mol}^{-1}$) is the molar mass of the electrode material, V_m ($\text{cm}^3\cdot\text{mol}^{-1}$) is the molar volume of the electrode material, S (cm^2) is the geometric area of the electrode, M_b/V_b can be derived from the density of the electrode material, L (cm) is the average thickness of the electrode. When the GITT plot shows a linear proportionality between voltage and $t^{1/2}$, Equation (S3) simplifies to:

$$D = \frac{4}{\pi\tau} \left(\frac{m_b V_m}{M_b S} \right)^2 \left(\frac{\Delta E_s}{\Delta E_\tau} \right)^2 \quad (\text{S4})$$

Using Equation (S4), the ionic diffusion coefficient can be calculated.

Material characterizations

X-ray diffraction (XRD) patterns were obtained by a Rigaku Ultra 250 detector with Cu K α radiation (1.5406 Å, 40 kV 40 mA). The diffraction peaks were recorded from 5° to 80° with an interval of 0.02° and a sweep rate of 10° min⁻¹. The morphologies and microstructures were collected by scanning electron microscopy (SEM, ZEISS, Gemini300S) and transmission electron microscopy (TEM, JEOL, JEM-2100F). The surface chemical and oxidation states of the electrode materials were analyzed by X-ray photoelectron spectroscopy (XPS, Perkin-Elmer PHI 550 spectrometer) with Al K α (1486.6 eV) as the X-ray source. The Fourier transform infrared spectroscopy (FT-IR) measurements were carried out on Shimadzu IR Prestige-21.

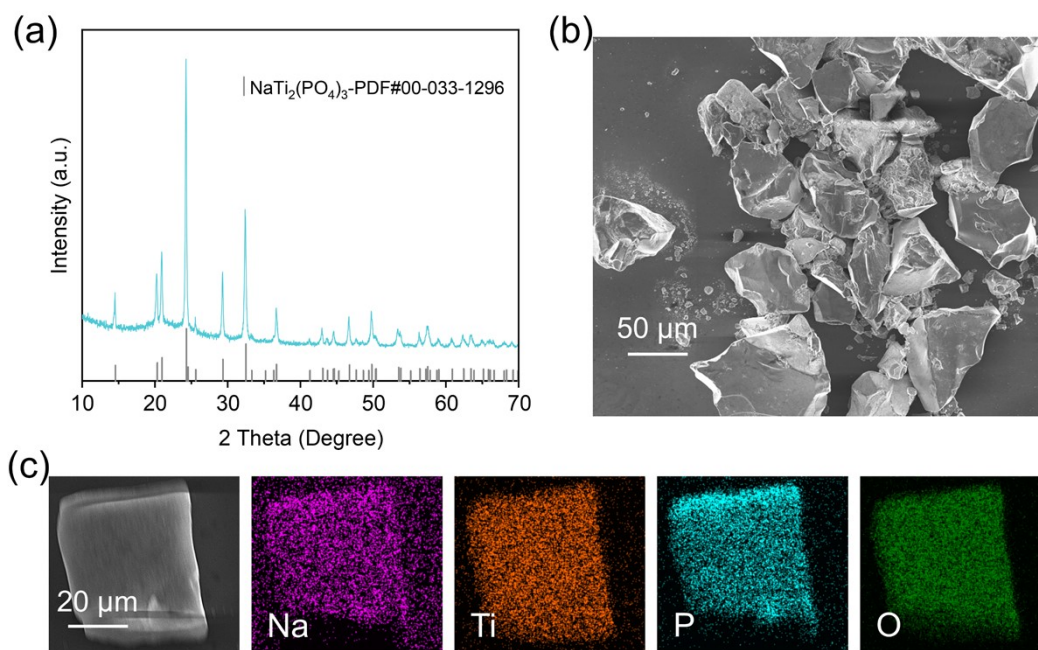


Fig. S1 Structural characterization of NTP material prepared by traditional method. (a) XRD pattern. (b) SEM image. (c) EDS mapping.

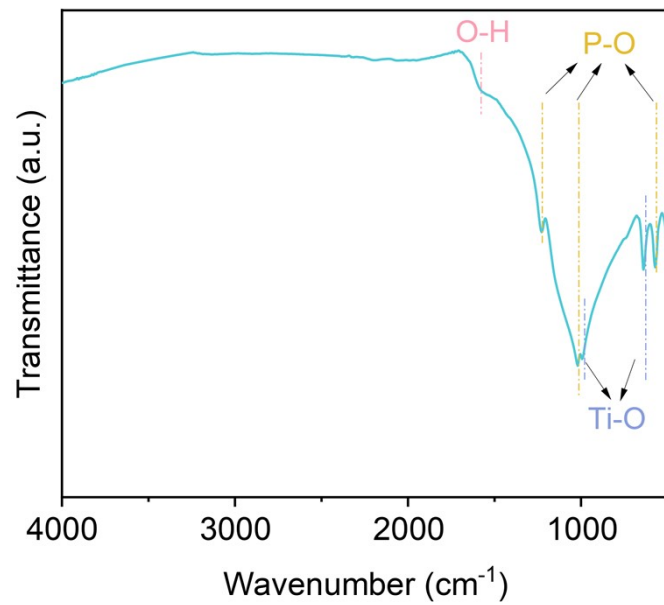


Fig. S2 The FT-IR spectrum of NTP.

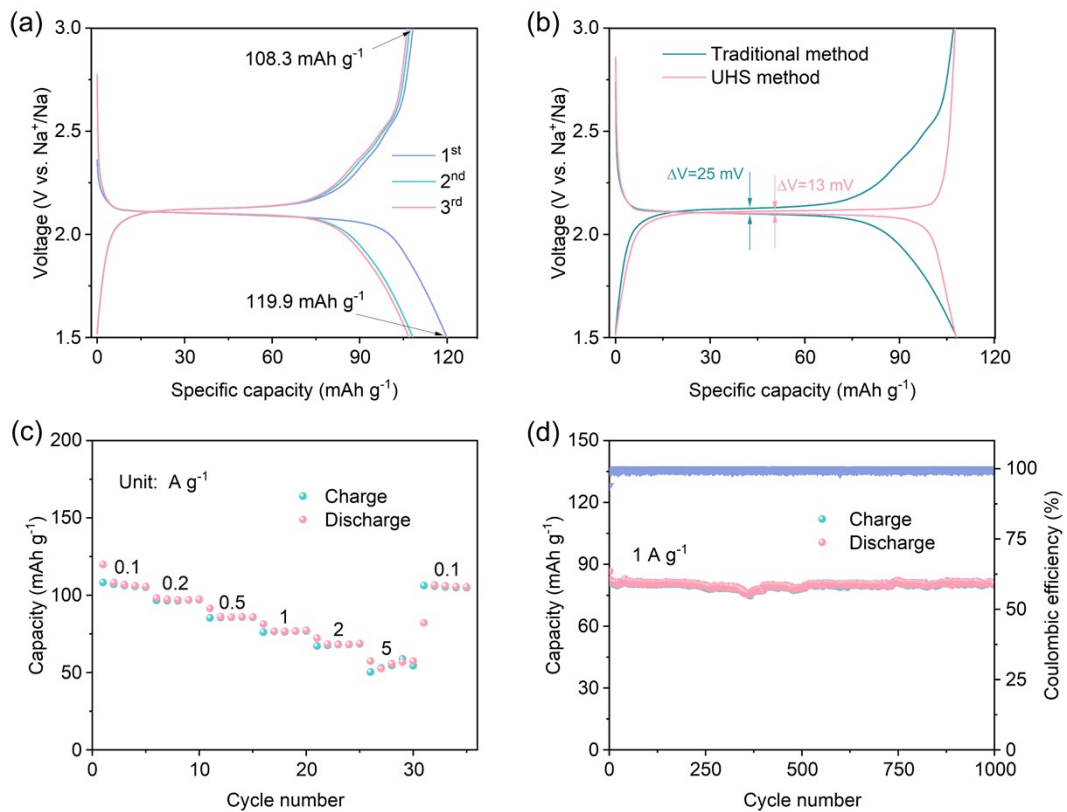


Fig. S3 Electrochemical performance of NTP prepared by traditional method. (a) The initial three GCD curves at 0.1 A g^{-1} . (b) Comparison of the second-cycle GCD curve of NTP prepared by two methods at 0.1 A g^{-1} . (c) Rate performance from 0.1 - 5.0 A g^{-1} . (d) Long-term cycle performance at 1.0 A g^{-1} .

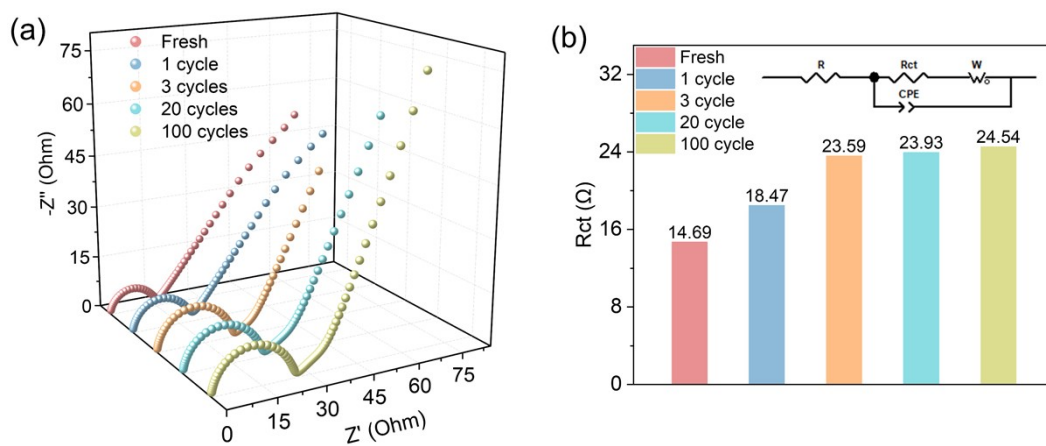


Fig. S4 (a) The EIS of NTP anode. (b) Charge transfer resistance (R_{ct}). Inset indicates equivalent circuit model.

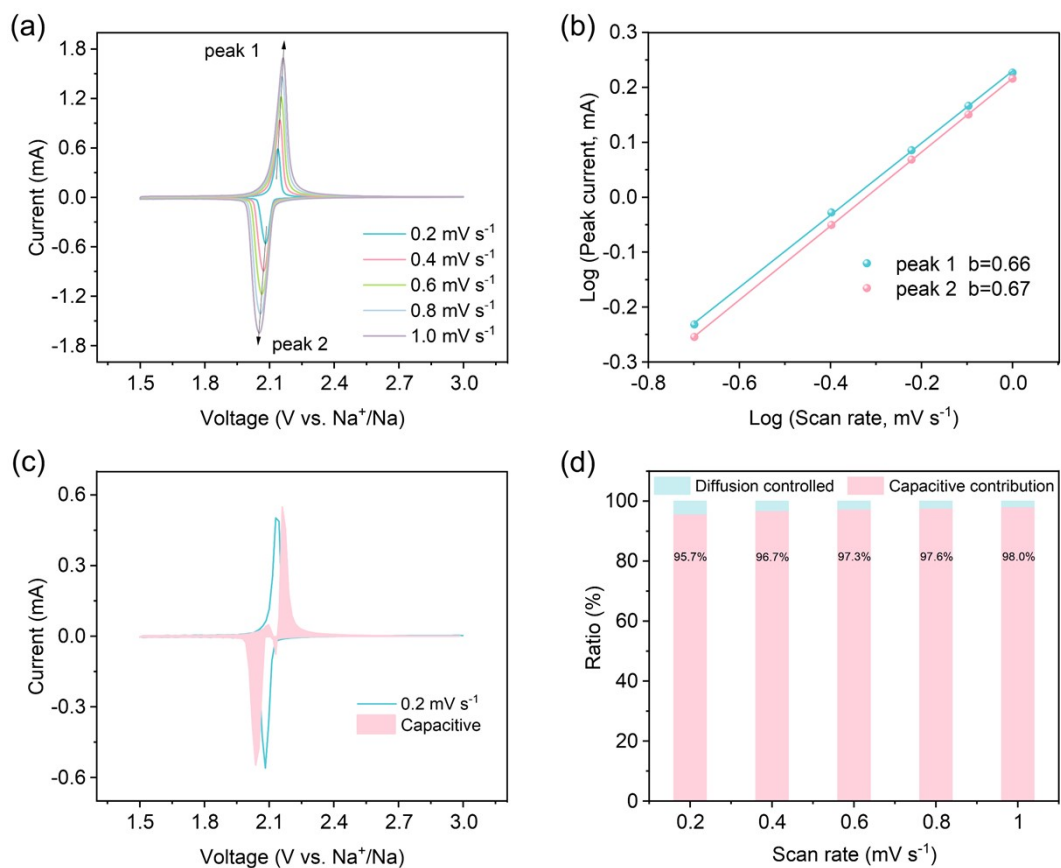


Fig. S5 Kinetics characterization. (a) CV curves at different scan rates of NTP anode. (b) Relationship between the logarithm peak current and logarithm scan rates. (c) Capacitive contribution and diffusion contribution at 0.2 mV s⁻¹. (d) The ratio of capacitive contribution at different scan rates.

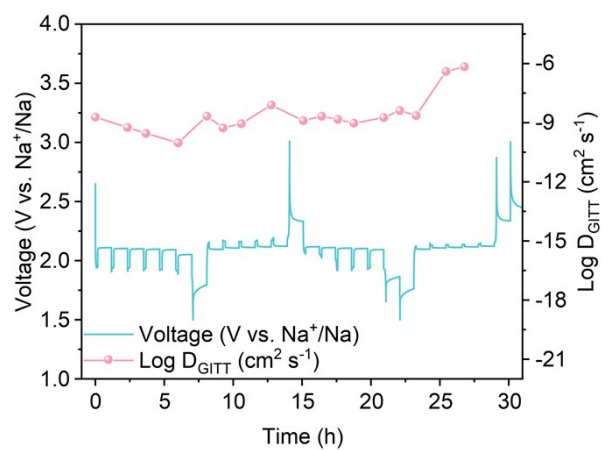


Fig. S6 Charge/discharge profiles and calculated D_{GITT} at first two cycles in the GITT measurements for NTP anode.

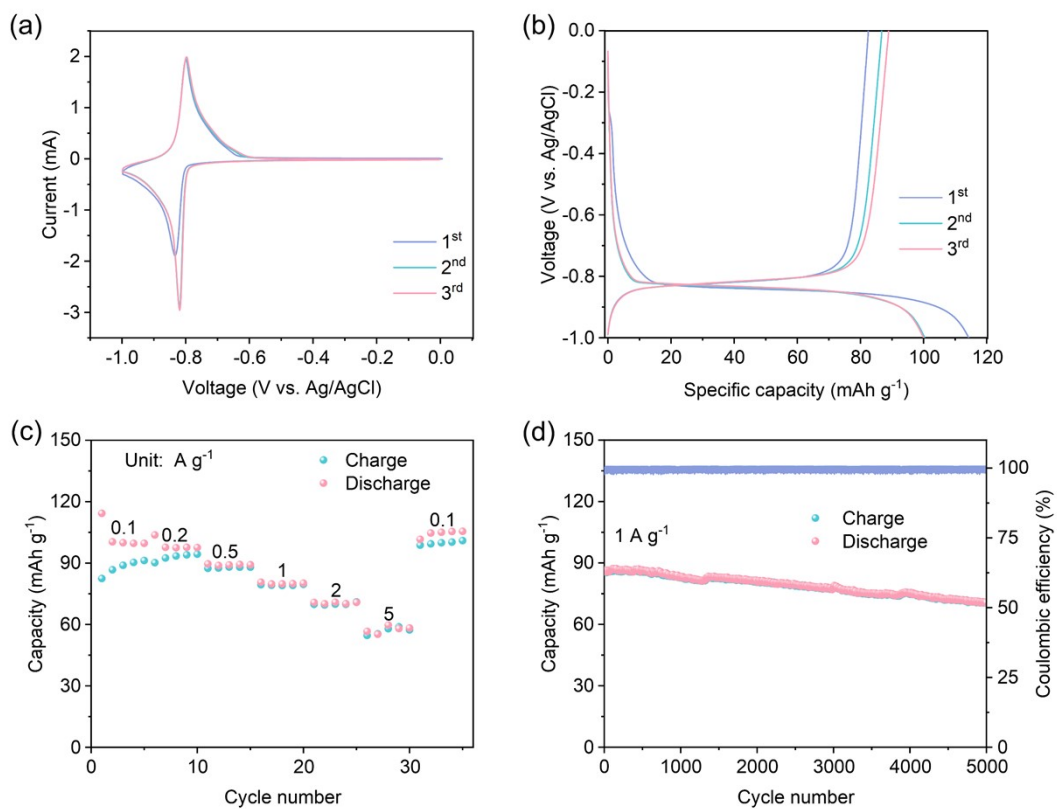


Fig. S7 Electrochemical performance of aqueous sodium-ion batteries of NTP anode. The initial three (a) CV curves at 1.0 mV s^{-1} and (b) GCD curves at 0.1 A g^{-1} . (c) Rate performance ranging from $0.1\text{-}5.0 \text{ A g}^{-1}$. (d) Long-term cycle performance at 1.0 A g^{-1} .

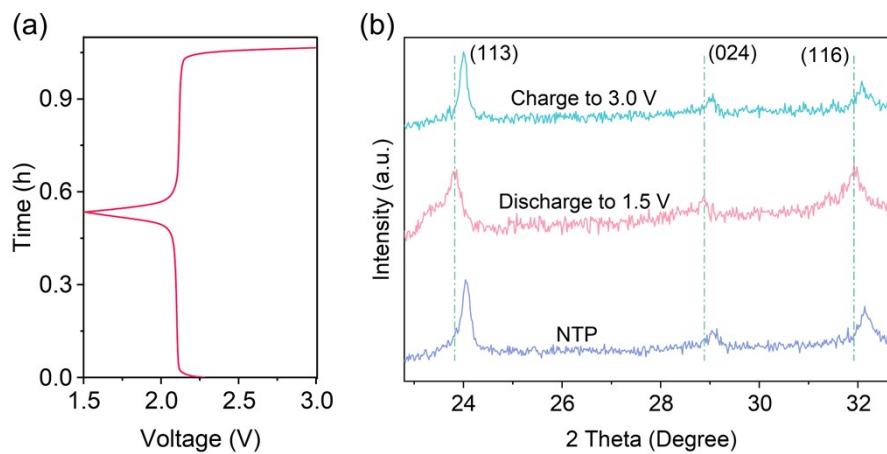


Fig. S8 (a) The GCD curves of NTP. (b) The ex-situ XRD of NTP.

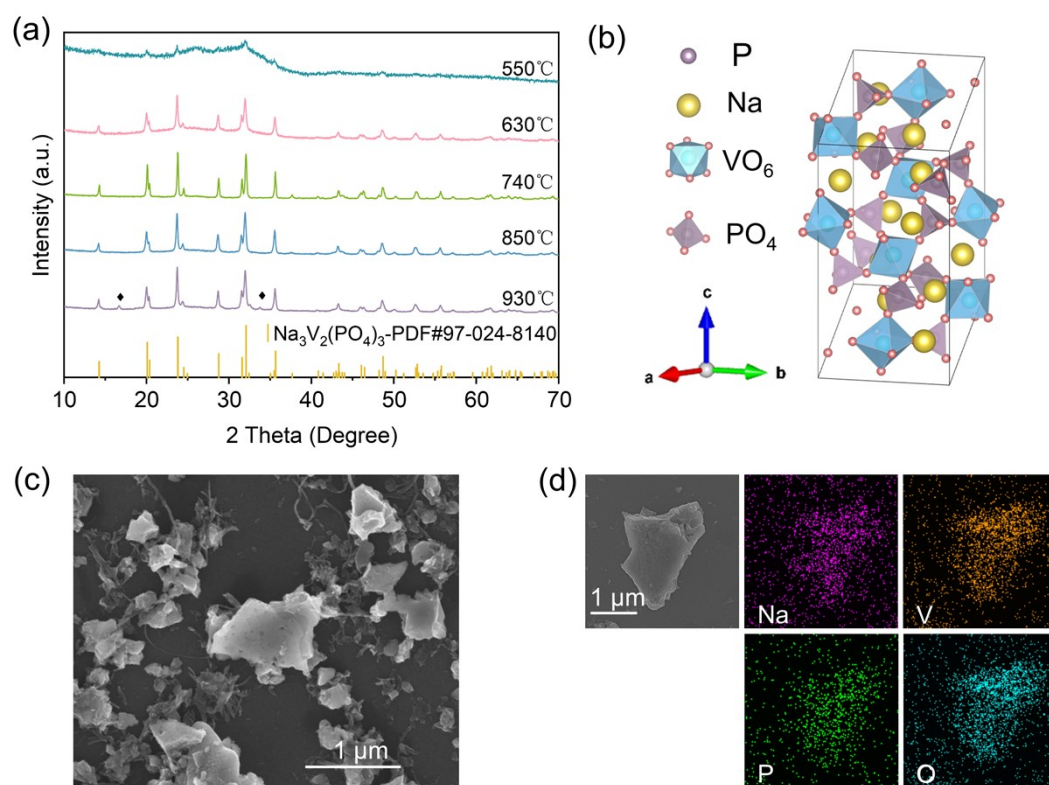


Fig. S9 Structural characterization of NVP material. (a) XRD patterns. (b) Crystal structure. (c) SEM image. (d) EDS mapping.

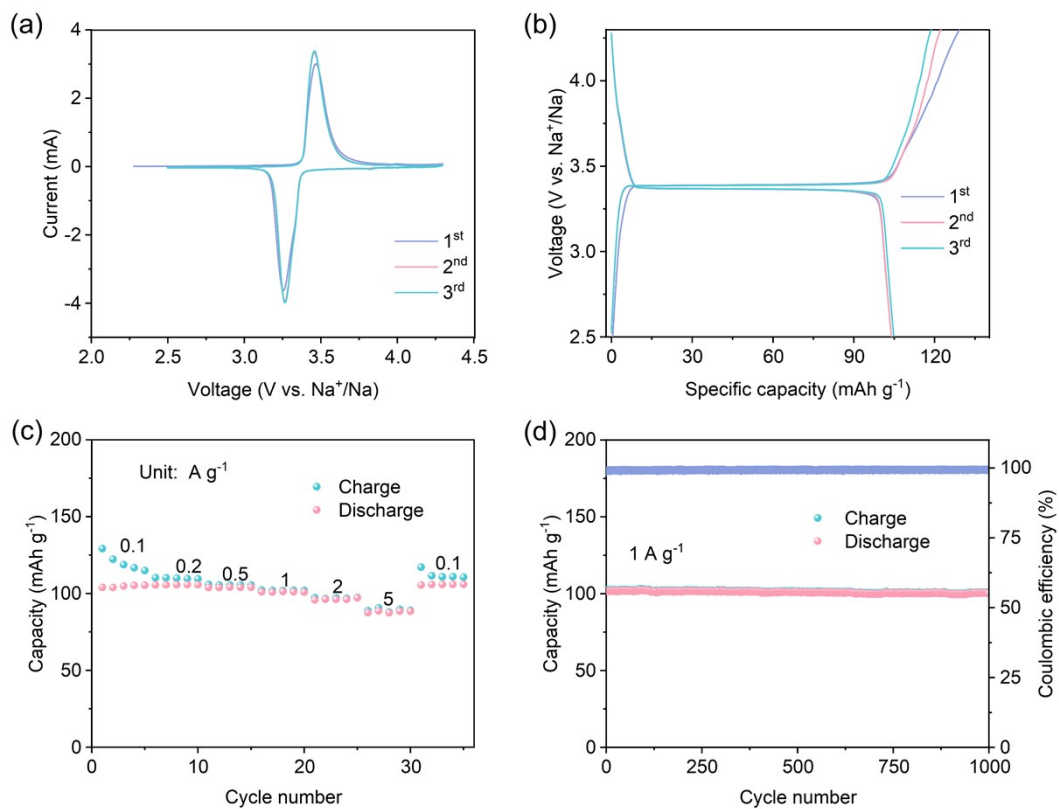


Fig. S10 Electrochemical performance of NVP cathode. The initial three (a) CV curves at 1.0 mV s^{-1} and (b) GCD curves at 0.1 A g^{-1} . (c) Rate performance ranging from 0.1 - 5.0 A g^{-1} . (d) Long-term cycle performance at 1.0 A g^{-1} .

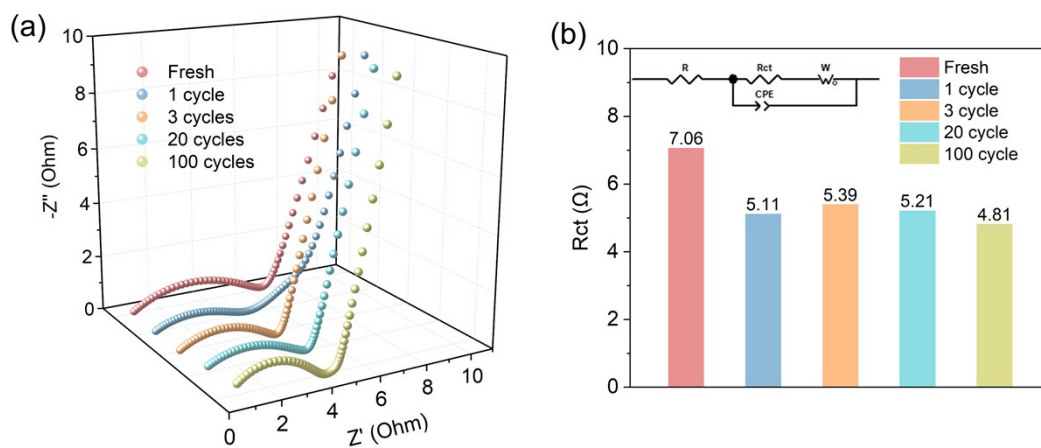


Fig. S11 (a) The EIS of NVP cathode. (b) Charge transfer resistance (R_{ct}). Inset indicates equivalent circuit model.

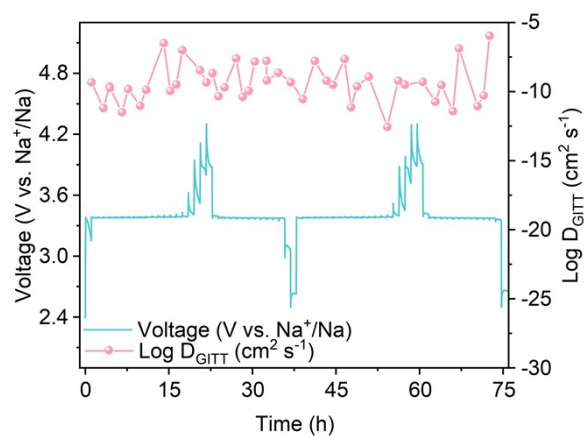


Fig. S12 Charge/discharge profiles and calculated D_{GITT} at first two cycles in the GITT measurements for NVP cathode.

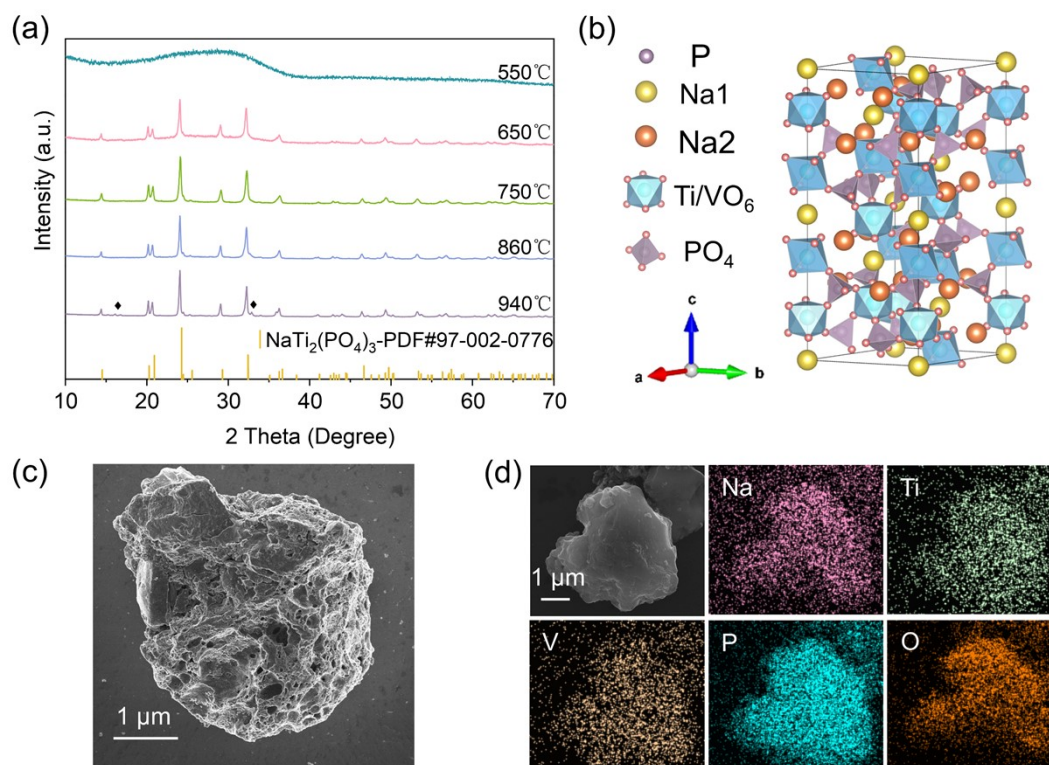


Fig. S13 Structural characterization of NVTP material. (a) XRD patterns. (b) Crystal structure. (c) SEM image. (d) EDS mapping.

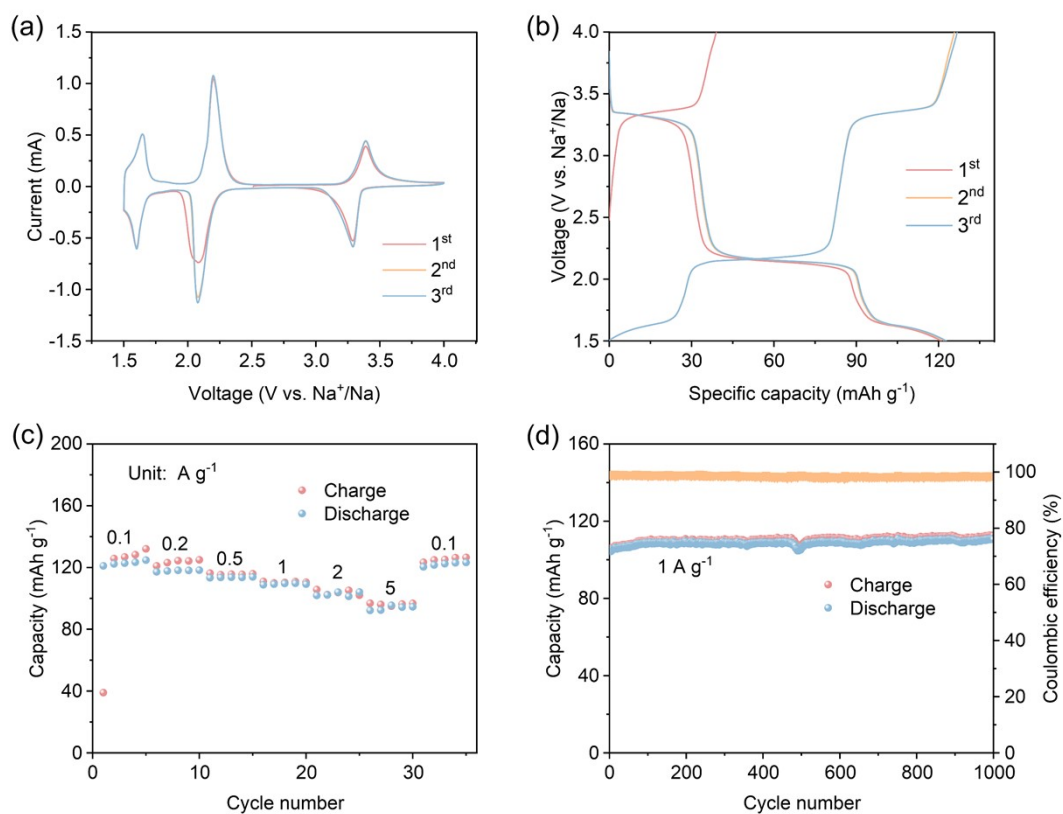


Fig. S14 Electrochemical performance of NVTP cathode. The initial three (a) CV curves at 1.0 mV s^{-1} and (b) GCD curves at 0.1 A g^{-1} . (c) Rate performance ranging from 0.1 - 5.0 A g^{-1} . (d) Long-term cycle performance at 1.0 A g^{-1} .

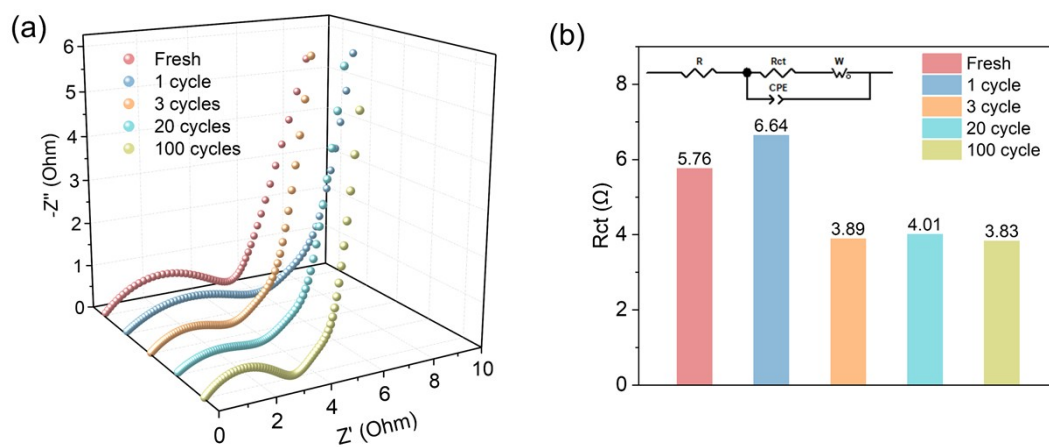


Fig. S15 (a) The EIS of NVTP cathode. (b) Charge transfer resistance (R_{ct}). Inset indicates equivalent circuit model.

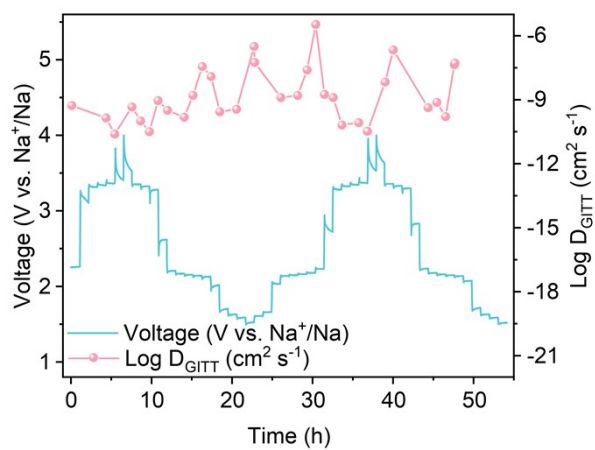


Fig. S16 Charge/discharge profiles and calculated D_{GITT} at first two cycles in the GITT measurements for NVTP cathode.

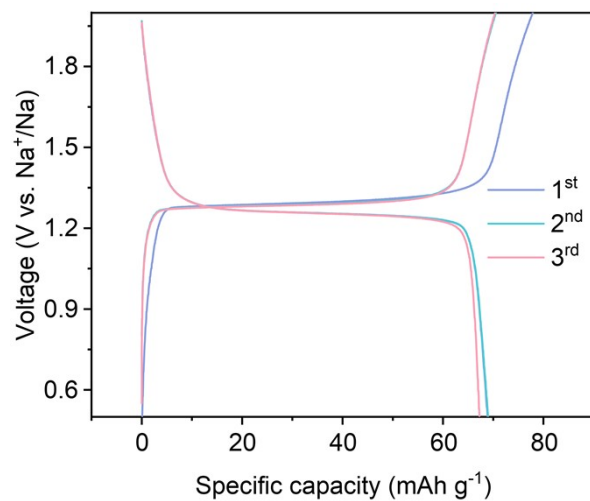


Fig. S17 The initial three GCD curves at 0.1 A g⁻¹ of the NVP//NTP full cell.